Localized Charge Distributions. III. Transferability and Trends of Carbon–Hydrogen Moments and Energies in Acyclic Hydrocarbons[1a]

Mark S. Gordon*[1b] **and Walter England**

Contribution from the Department of Chemistry and Institute for Atomic Research, Iowa State University, Ames, Iowa 50010. *Received July 3, 1971*

Abstract: The localized charge distributions defined previously are used to calculate INDO bond moments and energies of a variety of CH bonds in acyclic hydrocarbons. The polarity of all bonds discussed is C^+H^-. It is found that each basic type of CH bond (primary, vinyl, ethynyl) has an overflow of electron density (a "tail") out of the bond region which resides on and is characteristic of those atoms trans and coplanar to the bond. It is demonstrated that, since these tails are virtually independent of each other, the basic bond moments can be used to construct a model which predicts all calculated bond moments and orientations to a high degree of accuracy. While the total energies of the bonds e_i (where the molecular energy $E = \Sigma_i e_i$) are not very transferable, the intrabond and interference energies can be predicted rather well using a similar model. The trends in the bond moments are discussed in terms of the point charge and polarization contributions, and the interference energies are shown to correlate well with the trends in experimental CH bond energies. The trends in both properties are principally determined by the loss of interference density within the bond due to the presence of overflow atoms.

The ability to assign properties to the individual bonds of a molecule based on experimental or theoretical evidence is of considerable chemical interest. Bond multipole moments, for example, have been used for predicting and understanding internal rotation barriers[2] and intensities of normal modes of vibrations.[3] Further, if it is reasonable to assume that a particular bond undergoes only small changes when its chemical environment is slightly altered, then the properties of that bond should be transferable, at least in part, from one molecule to another and one might only need to assign bond properties for a small prototype of any homologous series. If, in addition, the net molecular property is expressible in terms of the various bond properties, one would then be able to predict the molecular properties of large molecules without laborious calculations.

Of particular concern in the present work are CH bond dipole moments and bond energies in hydrocarbons. Experimental bond moments may be obtained from intensities of the normal modes of vibrational spectra,[4] although Segal, *et al.*, have recently pointed out that these values may not be well defined.[5] The CH bond energies in a number of hydrocarbons have been determined by electron impact studies and have been collected in tabular form by Vedeneev and coworkers.[6] Theoretically, identification of bond properties is facilitated by the use of localized molecular orbitals (LMO's) since LMO's generally correspond to bonds, lone pairs, and inner shells.[7] The availability of LMO's enables one to construct localized charge distributions containing two electrons and two protons from which various properties may be derived.[8] In hydrocarbons these localized charge distributions correspond to CC or CH bonds or inner shells.

In order to study the transferability of theoretical bond properties from molecule to molecule, it is necessary to perform calculations on a rather large number of different types of molecules. Since *ab initio* SCF calculations are available for only a limited number of molecules, the semiempirical INDO method[9] was used to obtain the canonical molecular orbitals. It has been shown previously[10] that this method yields LMO's which are in good agreement with *ab initio* calculations.

In the first two papers of this series[8,11] it was found that localized orbitals have a certain amount of overflow of electrons (tails) out of the bond region which reside on those atoms trans and coplanar to the bond atoms. These tails were found to be important for the understanding of the barriers to internal rotation in ethane[8] and hydrogen peroxide.[11] One might expect that if properties of such bonds, or in fact the bond orbitals themselves, are to be transferable from molecule to molecule, such transferability should be dependent on these tails, and indeed we find this to be the case.

I. Method of Calculation

The details of the INDO method have been discussed elsewhere[9] and will not be repeated; however, a brief outline of the calculation of dipole moments within the INDO approximation follows. In the LCAO approximation, a molecular orbital (MO) φ_i (assumed real) is written

$$\varphi_i = \sum_\mu \chi_\mu C_{\mu i} \qquad (1)$$

---

[1] (a) Work performed in the Ames Laboratory of the Atomic Energy Commission, Contribution No. 3050. (b) Department of Chemistry, North Dakota State University, Fargo, N. D. 58102.

[2] E. M. Lassettre and L. B. Dean, *J. Chem. Phys.*, 17, 317 (1949).

[3] J. Overend, "Infrared Spectroscopy and Molecular Structure," M. Davies, Ed., Elsevier, Amsterdam, 1963.

[4] R. E. Hillier and J. W. Straley, *J. Mol. Spectrosc.*, **5**, 24 (1960).

[5] G. A. Segal, R. Bruns, and W. B. Person, *J. Chem. Phys.*, **50**, 3811 (1969).

[6] V. I. Vedeneev, L. V. Gurvich, V. N. Kondrat'ev, V. A. Medvedev, and E. L. Frankevich, "Bond Energies, Ionization Potentials, and Electron Affinities," Edward Arnold Publishing Co., New York, N. Y., 1966.

[7] C. Edmiston and K. Ruedenberg, *Rev. Mod. Phys.*, **35**, 457 (1963); *J. Chem. Phys.*, **43**, 597 (1965).

[8] W. England and M. S. Gordon, *J. Amer. Chem. Soc.*, **93**, 4649 (1971).

[9] J. A. Pople, D. L. Beveridge, and P. A. Dobosh, *J. Chem. Phys.*, 47, 2026 (1967).

[10] W. England and M. S. Gordon, *J. Amer. Chem. Soc.*, **91**, 6864 (1969).

[11] W. England and M. S. Gordon, *ibid.*, **94**, 4818 (1972).

where the χ_μ are atomic orbitals. The INDO electron density (inner shells are neglected in INDO) for a closed-shell system is

$$\rho = 2\sum_i^{\text{occ}}\varphi_i\varphi_i = \sum_\mu\sum_\nu P_{\mu\nu}\chi_\mu\chi_\nu \tag{2}$$

where i sums over all occupied MO's and P is the population matrix

$$P_{\mu\nu} = 2\sum_i^{\text{occ}}C_{\mu i}C_{\nu i} \tag{3}$$

In INDO each diagonal element of P is a total charge associated to the corresponding Slater orbital of the basis. The total (valence electron) charge associated with atom A is then

$$P_{\text{A}} = \sum_\mu^{\text{A}} P_{\mu\mu} \tag{4}$$

the summation including all orbitals on atom A. The X component of the molecular dipole moment (in debyes) is written[12]

$$\mu_X = 2.5416\sum_{\text{A}}(Z_{\text{A}} - P_{\text{A}})X_{\text{A}} - 14.674\sum_{\text{A}}^{*}(Z_{\text{A}}')^{-1}P(2\text{s}_{\text{A}},2\text{p}_{x_{\text{A}}}) \tag{5}$$

where Z_{A} is the core charge (nuclear charge plus inner shell electrons) on atom A, Z_{A}' is the orbital exponent for the L shell of atom A (obtained from Slater's rules), and $P(2\text{s}_{\text{A}},2\text{p}_{x_{\text{A}}})$ is the population matrix element between the 2s and 2p_x orbital on atom A. The second sum in eq 5 includes all atoms other than H. The first term in eq 5 is the contribution of the net charges at the nuclear positions, and the second sum is a *one-center* interference (or polarization) term[13] due to the wave properties of the electrons and represents the displacement of electrons away from the nuclear positions. Since we do not consider ions here, the contribution to the total moment from the net charges (point charges, pc) is origin invariant, as is the total contribution of the interference (sp) term. The latter invariance arises from the intraatomic orthogonality of the χ's: the interference term merely polarizes the density and makes no contribution to the population.

We use the Edmiston–Ruedenberg method of energy localization[7,14] in which the sum

$$D = \sum_i[ii|ii] = \sum_i\int \mathrm{d}V_1\int \mathrm{d}V_2\varphi_i^2(1)\varphi_i^2(2)(r_{12})^{-1} \tag{6}$$

is maximized against orthogonal transformations in the occupied MO space. The energy localized orbitals (LMO's) are defined as those MO's which maximize D. In all cases considered, D was constant to ten decimal places before localization was terminated. All molecular geometries were obtained from the standard model of Pople and Gordon.[12,15]

II. Bond Moments

For a closed-shell molecule in the MO approximation, the electronic contribution (μ_{el}) to the dipole moment is a sum of contributions from the individual MO's ($\mu_{\text{el}}(i)$)

$$\mu_{\text{el}} = \sum_i^{\text{occ}}\mu_{\text{el}}(i) \tag{7}$$

Equation 7 is a consequence of the orthonormality of the MO's and hence is true for any set of occupied MO's. In the localized representation, the nuclear charges may be partitioned[8] to form localized charge distributions $Z_i(\text{A})$; thus, the molecular dipole moment may be expressed as a vector sum of "bond" moments, *i.e.*, moments of the localized charge distributions. Since we consider neutral bonds only, two units of positive charge are assigned to each LMO

$$\sum_{\text{A}}Z_i(\text{A}) = 2 \tag{8}$$

To preserve the net core charges, we must also have

$$\sum_i Z_i(\text{A}) = Z_{\text{A}} \tag{9}$$

As shown in a previous paper (hereafter referred to as I),[8] eq 8 and 9 are satisfied if the positive charge is distributed as follows. (1) For an inner shell or lone pair on atom A, $Z_i(\text{A}) = 2$; $Z_i(\text{B}) = 0$ for all B $\neq$ A. (2) For a bond orbital between atoms A and B, $Z_i(\text{A}) = Z_i(\text{B}) = 1$; $Z_i(\text{C}) = 0$ for all C $\neq$ A and C $\neq$ B. If $P_i(\text{A})$ is the population on atom A in the LMO λ_i, then the bond moment of the ith localized charge distribution is

$$\mu_x(i) = 2.5416\sum_{\text{A}}[Z_i(\text{A}) - P_i(\text{A})]X_{\text{A}} - 14.674\sum_{\text{A}}^{*}(Z_{\text{A}}')^{-1}P_i(2\text{s}_{\text{A}},2\text{p}_{x_{\text{A}}}) \tag{10a}$$

or

$$\mu_x(i) = \mu_{\text{pc}}^x(i) + \mu_{\text{sp}}^x(i) \tag{10b}$$

where

$$P_i(2\text{s}_{\text{A}},2\text{p}_{x_{\text{A}}}) = 2C_{2\text{s}_{\text{A}}\text{A}.i}C_{2\text{p}_{x_{\text{A}}}.i} \tag{11}$$

and in terms of the bond moments

$$\mu_x = \sum_i^{\text{occ}}\mu_x(i) = \sum_i[\mu_{\text{pc}}^x(i) + \mu_{\text{sp}}^x(i)] \tag{12}$$

In hydrocarbons, the interference bond moment, $\mu_{\text{sp}}(i)$, has contributions only on the carbon atoms and, since the CH orbitals are localized, will be primarily determined by the bond carbon. For all CH bonds considered in the present work, the carbon hybrid is polarized such that the H is at the negative end of μ_{sp}. Since there is little charge separation in hydrocarbon CH bonds, μ_{pc} is small and the polarity of the *total* bond moment is also C^+H^-.

Saturated CH Bonds. The impetus for seeking transferable bond properties is the construction of a simple model for predicting the net molecular property. Such a model for bond moments must therefore specify not only the magnitude of the moment but its orientation in space as well.

Figure 1 defines a general primary CH bond ($\text{C}_\text{p}\text{H}$) for a hydrocarbon in which the carbon is bonded to a substituent X. Note that the bond moment, as mentioned in the preceding paragraph, is polarized C^+H^-. Φ is the angle μ makes with the CX bond

---

(12) J. A. Pople and M. Gordon, *J. Amer. Chem. Soc.*, **89**, 4253 (1967).

(13) K. Ruedenberg, *Rev. Mod. Phys.*, **34**, 326 (1962).

(14) C. Edmiston and K. Ruedenberg, "Quantum Theory of Atoms, Molecules, and the Solid State," P. O. Lowdin, Ed., Academic Press, New York, N. Y., 1966, p 263.

(15) M. Gordon and J. A. Pople, Quantum Chemistry Program Exchange, Program 135.

Table I. Model Moments and Angles for Primary Saturated CH Bonds[a]

Overflow atoms[b]	μ^{MOD}	$\Sigma\lvert\mu - \mu^{\mathrm{MOD}}\rvert/N$[c]	$\Delta\mu$[d]	Φ^{MOD}	$\Sigma\lvert\Phi - \Phi^{\mathrm{MOD}}\rvert/N$[c]	$\Delta\Phi$[e]
C_p–H (1)	1.956		−0.079	70.74		0.21
C_s–H (10)	1.967	0.002	−0.068	70.65	0.05	0.12
C_t–H (7)	1.975	0.004	−0.060	70.54	0.02	0.01
C_v–H (2)	1.976	0.005	−0.058	71.06	0.00	0.53
$(C–C)_{sat}$ (15)	1.991	0.004	−0.043	69.99	0.07	−0.54
C_v–C (2)	1.993	0.002	−0.041	70.36	0.03	−0.17
C–C_v (5)	1.991	0.004	−0.044	70.10	0.14	−0.43
C–C_e (2)	1.982	0.002	−0.052	70.34	0.04	−0.19
C=C (4)	1.900	0.006	−0.135	72.13 (1.0)	0.14	1.60
C≡C (2)	1.855	0.000	−0.175	74.27	0.11	3.74
C_p–H[f] (1)	1.980		−0.055	70.86		0.33
C_v–H[f] (1)	1.986		−0.048	69.97		0.56
C=C[f] (1)	1.940		−0.095	73.05 (−0.8)		2.52

[a] Moments in debyes, angles in degrees. [b] The subscript on a carbon indicates the type of carbon overflow atom: p = primary, s = secondary, t = tertiary, v = vinyl, e = ethynyl. The first atom in this column is the one directly bonded to the carbon of the CH bond. The number of prototypes is given in parentheses. [c] The average deviation from the model value. [d] $\Delta\mu = \mu^{\mathrm{MOD}} - \mu$(methane) where μ(methane) = 2.0348 D. [e] $\Delta\Phi = \Phi^{\mathrm{MOD}} - 70.53$ (all bonds tetrahedrally distributed). [f] Overflow atoms eclipsed to CH bonds.

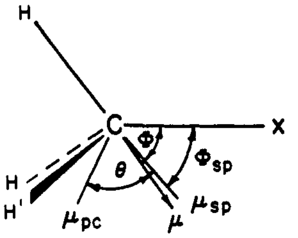

Figure 1. Definition of primary CH bond moment contributions.

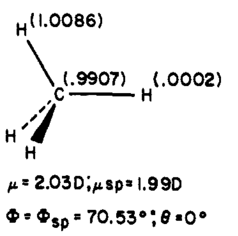

Figure 2. Atomic charge populations and bond moments for the CH bond in methane.

axis and similarly for Φ_{SP}. The angle between μ_{pc} and μ_{sp} is denoted by θ. In CH_4, μ coincides with the CH bond axis and Φ = 70.53°. The corresponding populations are shown in Figure 2. Note that the orbital is almost completely localized about the two bond atoms, there being a negligible electron population on the other hydrogens. The previously mentioned smallness of μ_{pc} is now apparent since the magnitude μ_{sp} is about 98% of μ.

Figure 3 contains the significant electron populations for C_pH bonds in a variety of molecular environments. The most striking difference between Figures 2 and 3 is that when a substituent is placed on the methyl carbon, the primary CH orbital is no longer as localized about the two atoms of the bond. Instead, there is a significant overflow of electron density onto other atoms in the molecule. This is the "overflow density" due to the tails of the localized orbitals which was found to be important in determining the internal rotation barriers for ethane[8] and peroxide.[11] For saturated CH bonds this overflow of electrons is only significant on pairs of atoms which are trans to and coplanar with the two atoms of the bond, *e.g.*, the C atoms adjacent to the first CH bond in propane (Figure 3). More important as far as transferability is concerned, the amount of overflow also varies with the type of "overflow atoms," and, in fact, *a primary CH bond may be categorized by its overflow atoms*, as is apparent in Table I. Approximately 40 acyclic hydrocarbons were investigated. For each type of overflow atom the number of prototype cases is listed in parentheses (the values for specific molecules are available on request). When the overflow atoms are C=C or C≡C, the orbitals connecting them are of banana type.[7,10] The number in parentheses in the C=C column is the angle between μ and the HCX plane defined by $[\vec{CH} \times \vec{CX}]$. In all other cases μ is in the HCX plane so that μ and Φ completely specify the moment. Columns 2 and 5 list the average bond moments (μ^{MOD}) and angles (Φ^{MOD}) for each type of overflow pair, while columns 3 and 6 list the corresponding average absolute deviations of the prototypes from the model values. The smallness of these deviations indicates a rather high degree of transferability of both μ and Φ. $\Delta\mu$ and $\Delta\Phi$ are defined by

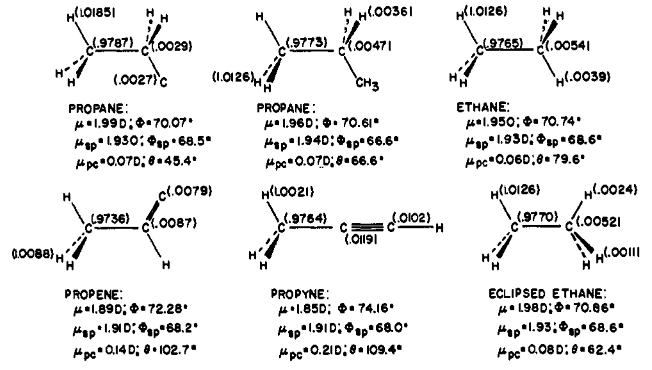

Figure 3. Atomic charge populations and bond moments for some primary CH bonds.

$$\Delta\mu = \mu^{\mathrm{MOD}} - \mu(CH_4) = \mu^{\mathrm{MOD}} - 2.0348\ \mathrm{D}$$

$$\Delta\Phi = \Phi^{\mathrm{MOD}} - \Phi(CH_4) = \Phi^{\mathrm{MOD}} - 70.53°$$

and are listed in columns 4 and 7 of Table I. In this way the model values are obtained from the parent molecule methane by adding deviations characteristic of the overflow atom pair. Note that all model moments are smaller than in methane. For completeness Table I lists model μ and Φ for three cases in which the overflow

Table II. Secondary CH Moments and Orientations[a]

Molecule	Overflow atoms (1)[b]	INDO Φ (1)	MOD Φ (1)	Overflow atoms (2)[b]	INDO Φ (2)	MOD Φ (2)	μ^{INDO}	μ^{MOD}
Propane	C_p–H	70.61	70.63	C_p–H	70.61	70.63	1.865	1.868
n-Butane	C_p–H	70.65	70.68	C_s–H	70.52	70.54	1.875	1.878
n-Pentane	C_p–H	70.63	70.68	C_s–H	50.57	70.54	1.877	1.878
n-Pentane	C_s–H	70.57	70.59	C_s–H	70.57	70.59	1.885	1.888
Isopentane	C_p–H	70.60	70.73	C_t–H	70.44	70.43	1.887	1.887
Isopentane	C_p–H	70.98	71.01	$(C–C)_{sat}$	69.90	69.88	1.904	1.903
s-trans-1-Pentene	C_p–H	70.63	70.68	C_s–H	70.46	70.54	1.880	1.878
1-Pentyne	C_p–H	70.60	70.68	C_s–H	70.58	70.54	1.862	1.878
s-trans-1-Butene	C_p–H	70.76	70.77	C═C	72.27	72.02	1.797	1.811
s-cis-1-Butene	C_p–H	68.73	68.83	C═C (cis)	72.88	72.94	1.856	1.852
s-trans-1-Pentene	C_s–H	70.67	70.68	C═C	72.31	72.07	1.808	1.821
1-Butyne	C_p–H	69.11	68.90	C≡C	73.91	74.16	1.773	1.771
1-Pentyne	C_s–H	69.05	68.81	C≡C	73.89	74.21	1.785	1.781
1,4-Pentadiene	C═C	70.37	70.22	C═C (cis)	73.00	73.08	1.796	1.795
1,4-Pentadiyne	C≡C	72.60	72.43	C≡C	72.60	72.43	1.676	1.674
Vinylethynylmethane	C═C	70.72	70.29	C≡C	74.14	74.30	1.715	1.714

[a] Moments in debyes, angles in degrees. [b] C_p, C_s, C_t indicates a primary, secondary, tertiary carbon, respectively.

Table III. Tertiary CH Moments and Orientations[a]

Molecule	Overflow atoms (1)	INDO Φ(1)	MOD Φ(1)	Overflow atoms (2)	INDO Φ(2)	MOD Φ(2)	Overflow atoms (3)	INDO Φ(3)	MOD Φ(3)	μ^{INDO}	μ^{MOD}
Isobutane	C_p–H	70.53	70.53	C_p–H	70.53	70.53	C_p–H	70.53	70.53	1.761	1.769
Isopentane	C_p–H	70.56	70.58	C_p–H	70.56	70.58	C_s–H	70.43	70.44	1.772	1.779
gauche-Isopentene	C_p–H	70.32	70.37	C_p–H	70.32	70.37	C_v–H	70.95	70.85	1.779	1.789
trans-Isopentene	C_p–H[b]	68.95	69.01	C_p–H	70.57	70.67	C═C	72.08	71.92	1.696	1.712
Isopentyne	C_p–H	68.91	68.79	C_p–H	68.91	68.79	C≡C	73.83	74.06	1.677	1.672

[a] Angles in degrees, moments in debyes. [b] Methyl group out of plane of vinyl group. [c] Methyl group in plane of vinyl group.

atoms are cis and coplanar to the CH bond. An example is eclipsed ethane (Figure 3), where it is seen that in this case the overflow is spread over *all* vicinal atoms.

The atomic populations in secondary CH bonds are illustrated in Figure 4. Just as the primary CH moments were found to be smaller than $\mu(CH_4)$, the secondary CH moments are generally smaller than $\mu(C_pH)$. There are two pairs of overflow atoms in secondary CH bonds, and comparison of Figures 3 and 4 implies that the overflow of electrons depends only on the overflow atoms themselves and very little on the surrounding molecular environments. This in turn suggests that the effects of pairs of overflow atoms on μ and Φ are virtually independent of each other. If this is the case, then for a secondary CH bond

$$\mu = \mu(CH_4) + \Delta\mu_1 + \Delta\mu_2 + \Delta\mu_{12} \qquad (13)$$

where $\Delta\mu_i$ is the standard change in the moment due to overflow pair i (Table I) and $\Delta\mu_{12}$ is the change in μ due to nonadditivity of overflow pairs and should be small. On the average, $\Delta\mu_{12}$ is -0.01 D. Assuming the Φ's to be independent and using $\Delta\mu_{12} = -0.01$ in all cases, we have calculated model moments and angles for secondary CH bonds. These are compared with those calculated directly from INDO LMO's in Table II, the agreement being generally quite good. Extending this treatment to tertiary bonds, we can generalize eq 13

$$\mu = \mu(CH_4) + \sum_i \Delta\mu_i + \sum_i \sum_{j<i} \Delta\mu_{ij} \qquad (14)$$

where, as before, the $\Delta\mu_i$ are taken from Table I and $\Delta\mu_{ij} = -0.01$ D. The model and calculated values of μ and Φ for tertiary CH bonds are compared in Table III where the predictive ability of the model is again apparent, and tertiary CH bond moments are seen to be still smaller than those of secondary bonds. These results confirm the suggested virtual independence of the effect of overflow atoms on bond moments in saturated CH bonds.

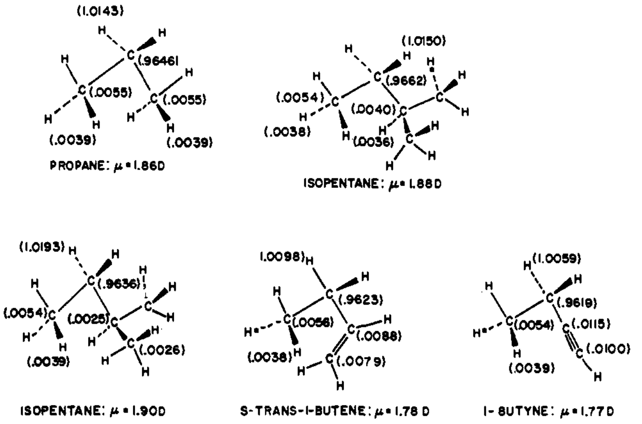

Figure 4. Atomic charge populations and bond moments for some secondary CH bonds.

Vinyl CH Bonds. The moments and orientations of vinyl CH bonds in monosubstituted ethylenes are defined in Figure 5. In each of the three possible types [cis (CH_c), trans (CH_t), and adjacent (CH_a) to the substituent], the H is again found to be at the negative end of the dipole. Φ, the angle between the moment and the C═C bond axis, would be 60° if the moment were coincident with the CH bond.

Atomic populations for the CH bond in ethylene are shown in Figure 6. All atoms in the molecule are significantly populated; however, the principal over-

Table IV. Model Moments and Angles for Vinyl CH Bonds[a]

Overflow atoms[b]	μ^{MOD}	$\Sigma\lvert\mu - \mu^{MOD}\rvert/N$[c]	$\Delta\mu$[d]	Φ^{MOD}	$\Sigma\lvert\Phi - \Phi^{MOD}\rvert/N$[c]	$\Delta\Phi$[e]
			I. H_t			
a. C_{sat} (12)	2.015	0.002	0.049	57.04	0.06	−0.68
b. C_v (2)	2.022	0.002	0.056	56.73	0.00	−0.94
c. C_e (1)	2.002		0.036	57.30		−0.37
			II. H_c			
a. C_{sat}, C_v (12)	1.993	0.003	0.027	57.45	0.07	−0.22
b. C_e (3)	1.976	0.001	0.010	57.39	0.07	−0.28
			III. H_a			
a. C_p–H (1)	1.891		−0.075	58.20		0.53
b. C_s–H (1)	1.899		−0.067	58.15		0.48
c. C_t–H (1)	1.907		−0.059	58.06		0.39
d. C_v–H (1)	1.890		−0.076	58.14		0.47
e. $(C–C)_{sat}$ (5)	1.921	0.003	−0.045	58.76	0.08	1.09
f. C–C_e (2)	1.913	0.002	−0.052	58.27	0.03	0.60
g. C≡C (1)	1.809		−0.157	56.20		−1.47
h. C_v–C (1)	1.931[f]		−0.034	58.19		0.52
i. C–C_v (1)	1.923[f]		−0.043	57.97		0.30
j. C_p–H (1)	1.911[f]		−0.055	58.10		0.43

[a] Moments in debyes, angles in degrees. [b] C_{sat}, C_p, C_s, C_t, C_v, C_e = saturated, primary, secondary, tertiary, vinyl, ethynyl carbon, respectively. Number of prototypes in parentheses. [c] Average deviations from model values. [d] $\Delta\mu = \mu^{MOD} - \mu$(ethylene). [e] $\Delta\Phi = \Phi^{MOD} - \Phi$(ethylene). [f] *s-cis*-vinyl group.

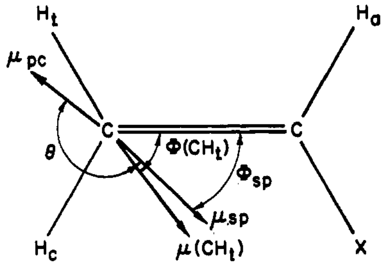

Figure 5. Definition of vinyl CH bond moments in monosubstituted ethylenes.

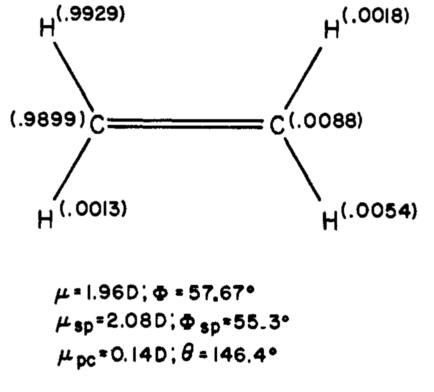

Figure 6. Atomic charge populations and bond moments for the ethylene CH bond.

flow atoms are once again those trans to and coplanar with the bond. Note that the moment is oriented behind the bond axis (Φ is less than 60°), reflecting the like displacement of the carbon hybrid of the bond.

Table IV lists the μ and Φ for CH_t, CH_c, and CH_a vinyl CH bonds, respectively, grouped according to type of overflow atoms. For each type, Δμ and ΔΦ are given by

$$\Delta\mu = \mu^{MOD} - \mu(\text{ethylene})$$

$$\Delta\Phi = \Phi^{MOD} - \Phi(\text{ethylene})$$

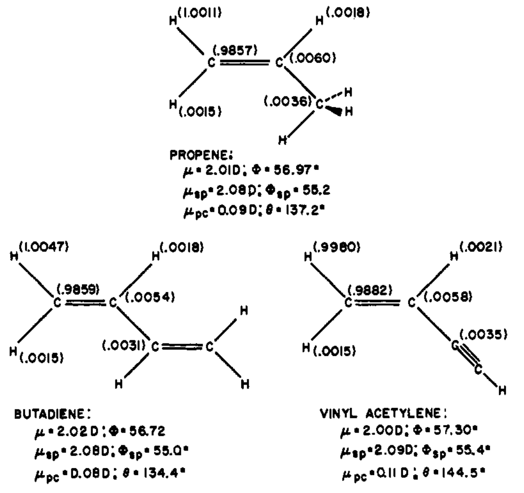

Figure 7. Atomic charge populations and bond moments for some CH bonds trans to the substituent in monosubstituted ethylenes.

For substituents trans or cis to the bond, μ is seen to be somewhat larger than for the parent molecule and rather less sensitive to changes in overflow atoms, whereas the variation in $\mu(CH_a)$ is quite similar to that found for saturated bonds with magnitudes generally smaller than μ(ethylene). For all three types, the degree of transferability is similar to that observed for primary CH bonds. It should be remarked that in all substituted ethylenes considered in this paper, the vinyl CH bonds lie in the plane of the vinyl group. Figures 7, 8, and 9 display the significant atomic populations in a number of CH_t, CH_c, and CH_a bonds, respectively.

Following the same procedure as for saturated systems, the average values for Δμ and ΔΦ listed in Table IV are used to predict the magnitudes and orientations of vinyl CH bonds in disubstituted ethylenes, the results being listed in Table V. Assuming

$$\Delta\mu = \mu(\text{ethylene}) + \Delta\mu_1 + \Delta\mu_2$$

$$\Delta\Phi = \Phi(\text{ethylene}) + \Delta\Phi_1 + \Delta\Phi_2$$

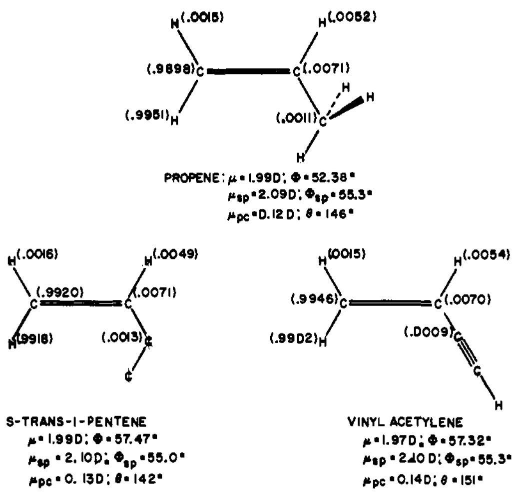

Figure 8. Atomic charge populations and bond moments for some CH bonds cis to the substituent in monosubstituted ethylenes.

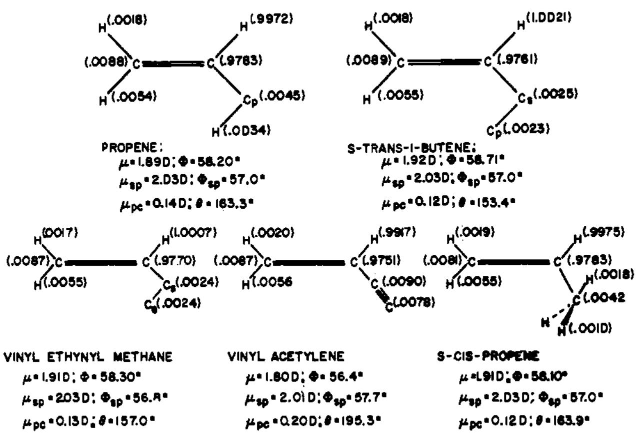

Figure 9. Atomic charge populations and bond moments for some CH bonds adjacent to the substituent in monosubstituted ethylenes. The C_p, C_s, and C_e stand for primary, secondary, and ethynyl carbons, respectively.

Table V. Comparison of Model and INDO Vinyl CH Moments in Disubstituted Ethylenes[a]

Molecule	Type[b]	μ(MOD)	μ(INDO)	Φ(MOD)	Φ(INDO)
2-Butene	IIa + IIIa	1.917	1.918	57.98	58.00
Isobutene	Ia + IIa	2.042	2.042	56.82	56.73
Isoprene[c]	Ia + IIa	2.042	2.041	56.82	56.76
Isoprene[d]	Ib + IIa	2.050	2.047	56.51	56.46

[a] Moments in debyes, angles in degrees. [b] Type refers to Table IV. [c] Vinyl H trans to methyl. [d] Vinyl H cis to methyl.

moments and angles are obtained to within 0.003 D and 0.09°, respectively, of the INDO values. Similar transferability is expected for trisubstituted ethylenes.

Ethynyl CH Bonds. The effect on the ethynyl CH bond of substituting various hydrocarbon groups is virtually independent of substituent. The bond moment in acetylene is 2.000 D, while the average C_eH moment for the eight-substituted acetylenes is 2.013 D. The moment is along the bond axis in all cases and the polarity is again C^+H^-.

Discussion

The trends in the bond moments discussed above can be understood in terms of the effect of different pairs of overflow atoms on the polarization (μ_{sp}) and point charge (μ_{pc}) contributions. Comparison of the CH bonds of propane (Figure 3) with the corresponding bond in CH_4 indicates that the overflow in the former molecule is obtained at the expense of the bonded carbon. In fact, there is a concurrent shift of electron population from the carbon to the hydrogen of the bond. μ_{sp}, being principally determined by the bond C, decreases as shown and is the major cause of the decrease in CH moments relative to methane. The point charge contribution, being small, is substantially affected by overflow of electron density out of the bond region as reflected by the large value of θ (45° in propane as opposed to 0° in methane). The net result is a smaller bond moment with an orientation closer to the bond axis. Since secondary and tertiary CH bonds add successive pairs of overflow atoms, their bond moments decrease even more.

It is also apparent from Figure 3 that the interference contributions to the CH moments are relatively insensitive to the *type* of overflow atoms. Thus, it can be concluded that *while the magnitude and orientation of primary CH bond moments are principally determined by the large interference contribution, differences among them are largely determined by the variation in the point charge contribution due to differing amounts of overflow.* The results listed in Tables II and III indicate that these effects are cumulative in secondary and tertiary CH bonds. Moreover, vinyl CH_a bond moments are subject to the same explanation, as can be seen from a comparison of Figures 6 and 9. For all the CH_a bonds, the overflow of electrons onto H_t, H_c, and the geminal vinyl carbon is virtually the same as for ethylene, the only differences arising from a source identical with that found for saturated bonds. This, then, explains why the moments of these bonds are smaller, and their orientations closer to the CH bond axis, than the corresponding moment in ethylene.

In contrast, the other two types of vinyl CH bonds (CH_t and CH_c) differ from ethylene only in the type of atom trans or cis to the bond in the vinyl group (Figures 7 and 8). Unlike the saturated CH bonds there is very little charge separation in the vinyl CH bond itself so that the point charge moment, μ_{pc}, is primarily determined by the overflow population. It has previously been remarked that trans-coplanar atoms receive the greatest amount of overflow and that trans hydrogens draw more overflow density than trans carbons. (See Figure 3.) It follows then that trans substitution for a hydrogen (CH_t) will decrease the overflow and thus increase the moment relative to ethylene. A similar substitution for a CH_c bond will have a similar, but smaller, effect since the cis hydrogen is a less important overflow atom. Finally, since the polarization contribution is virtually the same in CH_t and CH_c as it is in ethylene, we can conclude that the variations in these bond moments are primarily due to the introduction of a point charge moment which is characteristic of both the type and geometric position of the substituent. This explains the observed trends in the magnitudes of vinyl CH moments: $\mu(CH_a) < \mu(\text{ethylene}) < \mu(CH_c) < \mu(CH_t)$. Finally, as can be seen in Figure 10, all ethynyl bond moments are such that μ_{pc} directly opposes μ_{sp} so that $\mu = \mu_{sp} - \mu_{pc}$.

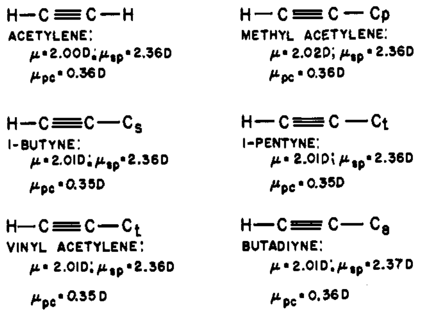

Figure 10. Atomic charge populations and bond moments for some ethynyl CH bonds.

Some of the gross results presented above were in fact predicted some time ago by Pople and Santry.[16] These authors constructed a set of completely localized bond orbitals within an extended-Hückel framework and then applied perturbation theory to determine the "degree of delocalization," or overflow, in localized orbitals. They predicted, as we have explicitly shown in the present work, that there is an inherent delocalization in *any* set of molecular orbitals, this delocalization, or overflow, in the case of localized orbitals being most prevalent in vicinal bonds, particularly in those vicinal bonds trans to and coplanar with the bond in question. It is now clear that *this overflow is in fact an inherent characteristic of the types of trans, coplanar bonds.* These authors also found the vinyl CH bond in ethylene to be delocalized over the entire vinyl group, the trans CH bond again being the most important. The present work shows this to be a general result for vinyl CH bonds in substituted ethylenes. Finally, Pople and Santry suggest that the ability to construct a model capable of predicting transferable bond properties depends on the ability of the model to account for these vicinal delocalizations in a consistent way. We feel that the localized orbitals presented here, characterized by their overflow atoms, provide just such an internally consistent vehicle.

LMO's and corresponding bond moments (calculated the same way we calculate ours) for some small hydrocarbons have recently been determined using *ab initio* wave functions.[17–20] These are compared with the INDO moments in Table VI. All theoretical moments are polarized C^+H^- and agree well with the INDO results except for the ethynyl CH bonds (acetylene and propyne). We also quote in Table XI the experimentally determined bond moment for deuterated methane.[4] As noticed previously,[17–21] there is considerable disparity between the experimental and theoretical values. In this regard, it has been suggested[17,18,21] that the experimental moment may in fact be the difference between the bond moment of the molecule and that of the separated atoms in hybridized valence states. Whatever the case, it is clear from Table VI that the bond moments we calculate are rather different from bond moments determined from vibrational spectroscopy. Of greater importance, however, is the ability to utilize bond moments to predict molecular dipole moments[12] without performing arduous calculations. The correlation with experimental values of dipole moments calculated using the similar CNDO/2 theory and the transferability of CH bond moments will satisfy the latter requirement.

Table VI. Comparison of INDO and *ab initio* Bond Moments (debyes)

Molecule	INDO	Rothenberg[a]	NSL[b]	Peters[c]	Exptl[d]
Methane	2.03	1.65	2.02	2.13	0.33
Ethane (staggered)	1.95		2.06		
Ethane (eclipsed)	1.97		2.04		
Propyne (methyl)	1.85		1.88		
Ethylene	1.96		1.92		
Acetylene	2.00		1.68		
Propyne (ethynyl)	2.02		1.70		

[a] Reference 17. [b] Reference 19. [c] Reference 20. [d] Reference 4.

III. Charge Distribution Energies

In paper I[8] it was shown that the total energy of a molecule can be written as the sum of the energies of the localized charge distributions, e_i

$$E = \sum_{i=1}^{N} e_i \qquad (15)$$

where N is the number of occupied MO's and, in INDO

$$e_i = U_i + \beta_i + \sum_{j=1}^{N} R_{ij} \qquad (16)$$

Letting M be the number of atoms

$$U_i = \sum_{A=1}^{M} U_i(A) \qquad (17)$$

is the one-electron, one-center quasiclassical energy of distribution i.

$$R_{ij} = V_{ij} + G_{ij} + g_{ij} \qquad (18)$$

contains the two-center quasiclassical electron–nucleus attraction energy (V_{ij}), the electron G_{ij}, and nuclear (g_{ij}) repulsion energies between distributions i,j; and

$$\beta_i = \sum_{A=1}^{M} \sum_{B \neq A} \beta_i(A,B) \qquad (19)$$

where β_i(A,B) is the one-electron, two-center interference energy between centers A and B in distribution i. The quantities U_i(A) and β_i(A,B) are derived from semiempirical parameters and therefore cannot be further partitioned.

Comparison with Experimental Bond Energies. The interference concept is part of a theory due to Ruedenberg, who stressed its importance first in a formal discussion of the chemical bond,[13] and later with coworkers, in applications to H_2O,[22] and certain first row diatomic hydride[23] and homonuclear[24] molecules. More recently, Moffat and Popkie[25] have found reasonable correlation between interference energies obtained

---

(16) J. A. Pople and D. P. Santry, *Mol. Phys.*, 7, 269 (1963); **9**, 301 (1965).

(17) S. Rothenberg, *J. Chem. Phys.*, **51**, 3389 (1969).

(18) R. H. Pritchard and C. W. Kern, *J. Amer. Chem. Soc.*, **91**, 1631 (1969).

(19) M. D. Newton, E. Switkes, and W. N. Lipscomb, *J. Chem. Phys.*, **53**, 2645 (1970).

(20) D. Peters, *ibid.*, **51**, 1566 (1969).

(21) W. C. Hamilton, *ibid.*, **26**, 345 (1957).

(22) C. Edmiston and K. Ruedenberg, *J. Phys. Chem.*, **68**, 1628 (1964).

(23) E. M. Layton, Jr., and K. Ruedenberg, *ibid.*, **68**, 1654 (1964).

(24) R. R. Rue and K. Ruedenberg, *ibid.*, **68**, 1676 (1964).

(25) J. B. Moffat and H. E. Popkie, *Int. J. Quantum Chem.*, **2**, 565 (1968).

Table VII. Comparison of Experimental Bond Energies with β_i (CH)[a]

Molecule	Type[c] of attached atoms	D_{CH}[d]	$-\beta_i$(CH)	$D_{CH} - \tilde{D}_{CH}$[e]	$-[\beta_i$(CH) $- \tilde{\beta_i}$(CH)]
I. Primary CH Bonds[b]					
Methane	H	4.40	20.617	0.00	0.00
Ethane	C_p	4.21	20.437	−0.19	−0.18
Propane	C_s	4.22	20.459	−0.18	−0.16
n-Butane	C_s	4.28	20.458	−0.12	−0.17
Propene	C_v	3.34	20.390	−1.06	−0.23
Isobutene	C_v	3.37	29.396	−1.03	−0.22
2-Butene	C_v	3.24	20.389	−1.16	−0.23
Propyne	C_e	≤3.49	20.279	≤−0.91	−0.34
II. Secondary CH Bonds[b]					
Propane	C_p, C_p	3.98	20.244	−0.42	−0.37
n-Butane	C_p, C_s	3.95	20.270	−0.45	−0.33
III. Tertiary CH Bonds					
Isobutane	C_p, C_p, C_p	3.93	20.035	−0.47	−0.58
IV. Unsaturated CH Bonds					
Ethylene		4.51	20.873	0.11	0.26
Acetylene		4.90	21.586	0.50	1.24

[a] All energies in electron volts. [b] When three hydrogens in a methyl group or two in a methylene group have different overflow atoms, the entries in this column are averaged values. [c] Type of atom(s) other than hydrogens to which carbon of CH bond is attached. [d] See ref 6. All experimental values have been reduced to 0°K. [e] The ~ indicates methane.

Table VIII. Model R_{ii} and β_i(CH) in Primary CH Bonds (eV)[a]

Overflow atoms[b]	R_{ii}^{MOD}[c]	$\Sigma\lvert R_{ii} - R_{ii}^{MOD}\rvert$[d]$/N$	ΔR_{ii}^{MOD}[c]	β_i^{MOD} (C,H)[c]	$\Sigma\lvert\beta_i(C,H) - \beta_i^{MOD}(C,H)\rvert$[d]$/N$	$\Delta\beta_i^{MOD}$(C,H)[c]
C_pH (1)	5.077		−0.107	−20.437		0.180
C_sH (10)	5.088	0.002	−0.096	−20.463	0.001	0.154
C_tH (7)	5.101	0.001	−0.083	−20.484	0.002	0.133
C_vH (2)	5.093	0.003	−0.091	−20.488	0.001	0.129
CC (24)	5.122	0.003	−0.062	−20.465	0.012	0.152
C=C (4)	5.024	0.008	−0.161	−20.355	0.013	0.262
C≡C (2)	4.952	0.002	−0.232	−20.278	0.001	0.339

[a] $R_{ii}(CH_4)$ = 5.184; β_i(C,H) in methane = −20.617 eV. [b] Number of prototypes in parentheses. [c] As defined in text. [d] Average deviation from model values.

from *ab initio* calculations on linear nitriles and corresponding experimental dissociation energies, while Fischer and Kollmar[26] related the $\beta(A,B)$ $(=\Sigma_i\beta_i(A,B))$ obtained from CNDO calculations to experimental trends in hydrocarbon bond energies with some success.

Since in an LMO representation most of the one-electron interference energy between bonded atoms A,B is contained in the interference energy of "bond" A–B, it is of interest to compare the β_i(CH) calculated for CH bonds in hydrocarbons with the corresponding experimental bond energies. Such a comparison is shown in Table VII (we actually quote $-\beta_i$(CH) in the tables). As one might expect, the magnitudes of β_i(CH) and the experimental D_{CH} are quite different; however, the more pertinent comparison is contained in the last two columns, which list the trends in the experimental and theoretical energies, respectively. Here the correlation is generally good. Methane is correctly predicted to have a bond energy larger than any other saturated CH bond and the trends D_{CH}(primary) > D_{CH}(secondary) > D_{CH}(tertiary), and D_{CH}(acetylene) > D_{CH}(ethylene) > D_{CH}(ethane) are properly reproduced. In addition, a CH bond in a methyl group attached to an unsaturated carbon (*e.g.*, propene, propyne) is correctly predicted to have a smaller bond energy than a similar bond attached to a saturated carbon (*e.g.*, propane), but the calculated difference is considerably smaller than observed. *These variations in β_i (CH) within a given type of CH bond (saturated, vinyl, or ethynyl) as well as variations from one type to another are directly due to changes in the interference density within the CH bond.* This follows from

$$\beta_i(\mathrm{CH}) = 2\sum_{\mu}^{\mathrm{C}}\sum_{\gamma}^{\mathrm{H}}P^i_{\mu\gamma}S_{\mu\gamma}\beta^0_{\mathrm{CH}} \qquad (20)$$

where β^0_{CH} is a semiempirical parameter dependent only on the atom pair, C,H. We point out that in Table VII the quoted values for β_i(CH) for primary and secondary CH bonds were obtained by averaging over the three (two) CH bonds in the methyl (methylene) group.

Transferability. Examination of the bond distribution energies (e_i) quickly dispels any idea of transferring them from molecule to molecule. Very little regularity is found. For example, the two primary CH bonds having overflow atoms C_tH in isopentane have bond distribution energies differing by more than 12 kcal. This is not surprising since the e_i contain electrostatic interactions between the bond in question and all other bonds, and these are sensitive to the number, type, and geometrical arrangement of bonds in the molecule. It is more likely that the *intra*distribution energies are regular. In INDO we can only directly calculate the contribution of R_{ii} (eq 18) to this quantity. In addition, since the β_i(C,H) are apparently related to C–H bond energies, it is of interest to determine the extent to which these can be characterized by the overflow atoms of the bond. The average R_{ii} and β_i(C,H) for primary CH bonds are listed in Table VIII according to type of

---

(26) H. Fischer and H. Kollmar, *Theor. Chim. Acta*, **16**, 163 (1970).

Table IX. Energy Components of Secondary and Tertiary CH Bonds (eV)

Molecule	Overflow atoms	R_{ii}	R_{ii}^{MOD}	$-\beta_i$(C,H)	$-\beta_i(\mathrm{C,H})^{\mathrm{MOD}}$
Propane	C_pH, C_pH	4.967	4.970	20.244	20.257
n-Butane	C_pH, C_sH	4.982	4.981	20.270	20.283
n-Pentane	C_pH, C_sH	4.982	4.981	20.272	20.283
	C_sH, C_sH	4.997	4.992	20.295	20.309
Isopentane	C_pH, C_tH	4.995	4.994	20.293	20.304
	C_pH, CC	5.018	5.015	20.287	20.285
s-trans-1-Butene	C_pH, $C{=}C$	4.897	4.917	20.149	20.175
s-trans-1-Pentene	C_sH, $C{=}C$	4.912	4.928	20.176	20.201
	C_pH, C_sH	4.978	4.981	20.273	20.283
1-Butyne	C_pH, $C{\equiv}C$	4.848	4.845	20.095	20.098
1-Pentyne	C_pH, $C{\equiv}C$	4.865	4.856	20.122	20.124
	C_sH, C_sH	4.977	4.992	20.269	29.309
Vinylethynylmethane	$C{=}C$, $C{\equiv}C$	4.789	4.792	20.009	20.016
1,4-Pentadiyne	$C{\equiv}C$, $C{\equiv}C$	4.723	4.720	19.940	19.939
Isobutane	C_pH, C_pH, C_pH	4.852	4.863	20.035	20.077
Isopentane	C_pH, C_pH, C_sH	4.867	4.874	20.060	20.103
s-gauche-Isopentene	C_pH, C_pH, C_vH	4.874	4.879	20.090	20.129
s-trans-Isopentene	C_pH, C_pH, $C{=}C$	4.780	4.810	19.942	19.995
1-Pentyne	C_pH, C_pH, $C{\equiv}C$	4.739	4.738	19.893	19.918
1,1-Vinylethynylethane	C_pH, $C{=}C$, $C{\equiv}C$	4.679	4.685	19.808	19.836

Table X. Model R_{ii} and β_i(CH) for Vinyl CH Bonds[a]

Overflow atoms[b]	R_{ii}^{MOD}	$\Sigma\lvert R_{ii} - R_{ii}^{\mathrm{MOD}}\rvert^c/N$	$\Delta R_{ii}^{\mathrm{MOD}\ d}$	$-\beta_i^{\mathrm{MOD}}$(C,H)	$\Sigma\lvert\beta_i(\mathrm{CH}) - \beta_i^{\mathrm{MOD}}(\mathrm{CH})\rvert^c/N$	$\Delta\beta_i^{\mathrm{MOD}}(\mathrm{C,H})^d$
I. H_t						
a. C_{sat} (11)	5.098	0.002	0.050	20.894	0.002	−0.021
b. C_v (2)	5.108	0.001	0.060	20.894	0.000	−0.021
c. C_e (1)	5.095		0.047	20.902		−0.029
II. H_c						
a. C_{sat}, C_v (11)	5.071	0.008	0.023	20.919	0.007	−0.046
b. C_e (3)	5.064	0.007	0.016	20.918	0.000	−0.047
III. H_a						
a. C_pH (1)	4.974		−0.074	20.738		0.135
b. C_sH (1)	4.985		−0.063	20.754		0.119
c. C_tH (1)	4.995		−0.053	20.771		0.102
d. C_vH (1)	4.972		−0.076	20.739		0.134
e. C–C (5)	5.008	0.003	−0.040	20.760	0.005	0.113
f. C–C_e (2)	5.008	0.003	−0.040	20.768	0.006	0.105
g. $C{\equiv}C$ (1)	4.884		−0.164	20.631		0.242

[a] Energies in electron volts. [b] Number of prototypes in parentheses. [c] Average deviation from model value. [d] $\Delta X[X = R_{ii}, \beta_i(\mathrm{C,H})] = X - X(\mathrm{ethylene})$; R_{ii}(ethylene) = 5.048 eV; β_i(C,H)(ethylene) = −20.873 eV.

overflow atoms. The four different types of C–C overflow atoms (C–C, C–C_v, C_v–C, C–C_e) are virtually indistinguishable and have been grouped together under the common heading C–C. Both quantities are quite regular as is evidenced by the quoted deviations. This transferability is encouraging, for we can now proceed as in section II to construct a model based on the primary CH bonds and make predictions for secondary and tertiary CH bonds. We define

$$\Delta R_{ii}^{\mathrm{MOD}} = R_{ii}^{\mathrm{MOD}} - R_{ii}(\mathrm{CH_4}) \qquad (21)$$

as the model deviation of R_{ii} from that of methane. For secondary and tertiary bonds

$$R_{ii}^{\mathrm{MOD}} = R_{ii}(\mathrm{CH_4}) + \sum_{i=1}^{P} \Delta R_{ii}^{\mathrm{MOD}} \qquad (22)$$

where the summation is over pairs of overflow atoms and the model values for β_i(CH) are defined similarly. $\Delta R_{ii}^{\mathrm{MOD}}$ and $\Delta\beta_i^{\mathrm{MOD}}$ (C,H) are listed in columns 3 and 7 of Table VIII. The model and calculated energy quantities for secondary and tertiary CH bonds are compared in Table IX. Both the R_{ii} and β_i(C,H) are well reproduced, indicating once again the virtual independence of different pairs of overflow atoms in the same bond. For secondary CH bonds the model R_{ii} and β_i(C,H) values are off by no more than 0.03 and 0.04 eV, respectively. The corresponding limits for tertiary CH bonds are 0.04 and 0.05 eV. Moreover, the trends in both quantities are in excellent agreement with those calculated directly with INDO. Based on the results presented in the beginning of this section, this implies that the model β_i(C,H) should be useful for predicting relative CH bond energies in larger hydrocarbons.

An understanding of the relative stabilities of the saturated CH bonds is now possible. *The CH bond in methane is most stable because there is virtually no overflow, and similarly* β_i *(primary CH)* < β_i*(secondary CH)* < β_i*(tertiary CH) because there are more overflow atoms in tertiary systems, less in secondary systems, and less yet in primary systems.* Since interference densities make no contribution to total populations, some care must be taken with this interpretation.[13] Thus, an increase (decrease) in the interference density between the bonded atoms does not necessarily follow a decrease (increase) in the overflow population. However, one would expect the observed correlation intuitively since, the greater the overflow, the less electrons are available for binding. Applications to cases where very small changes in overflow population occur are expected to be somewhat tenuous though.

Table X contains R_{ii} and β_i(CH) for CH$_t$, CH$_c$, and CH$_a$ bonds in monosubstituted ethylenes. The molecules are grouped in the same way as the corresponding bond moments (see section II) and both quantities are again seen to be rather transferable within a given group. Examination of these tables reveals that whereas substitution trans (CH$_t$) or cis (CH$_c$) to a CH bond in ethylene increases the bond energy slightly, substitution adjacent to the bond (CH$_a$) results in a considerable decrease in $-\beta_i$(CH). This parallels the behavior observed for bond moments, being due to the same effect: an increase in overflow results in less constructive interference between the bonded atoms.

Vinyl CH energies for some disubstituted ethylenes are shown in Table XI. Also tabulated are comparisons between the directly calculated values of R_{ii} and β_i(CH) with those obtained using the average values from Table X. The two sets of energies are in rather good agreement. Here, too, the trends may be explained in terms of the overflow, but both substituents must be considered.

Table XI. Energy Components of Vinyl CH Bonds in Disubstituted Ethylenes[a]

Molecule	Type[d]	R_{ii}	R_{ii}^{MOD}	$-\beta_i$(CH)	$-\beta_i^{\mathrm{MOD}}$ (CH)
2-Butene	IIa + IIIa	5.008	4.997	20.794	20.784
Isobutene	Ia + IIa	5.124	5.121	20.945	20.960
Isoprene[b]	Ia + IIa	5.126	5.121	20.951	20.960
Isoprene[c]	Ib + IIa	5.132	5.131	20.941	20.960

[a] Energies in eV. [b] Vinyl CH trans to methyl. [c] Vinyl CH cis to methyl. [d] Type refers to Table X.

The behavior of ethynyl CH bonds is similar to that observed for the moments. For acetylene, R_{ii} = 5.162 eV and β_i(C,H) = 21.711 eV while the average values for nine substituted acetylenes (5.174, $-$21.719 eV) are virtually independent of substituent.

IV. Trends in Overflow Population

We have found that *trends* in bond moments and bond energies for a *given type* of CH bond (saturated, vinyl, ethynyl) are predictable from the overflow population onto the "bond" coplanar with and trans (or cis in some cases) to the bond in question. Thus, it was possible to consider the standard systems methane (saturated), ethylene (vinyl), and acetylene (ethynyl) and interpret the trends as deviations from them. For example, there is no overflow bond in methane, and therefore all substituted methanes have a lower bond moment and weaker bond energy than does methane. Or, in staggered ethane the overflow bond is a CH bond, while in propane (for a primary CH bond) it may be either a CC or CH bond; and since the CC overflow is less than CH overflow, the (averaged) CH bond moment and energy are slightly higher in magnitude than for ethane.

In view of this important role played by the overflow populations, we now rank explicitly the pairs of overflow atoms for CH bonds in monosubstituted hydrocarbons according to the amount of population they acquire at the expense of the bonded atoms.

In saturated hydrocarbons the populations on the overflow atoms increase in the order C–C < C–H < C=C < C≡C. For vinyl CH bonds, as noted previously, the overflow populations increase from CH$_t$ to CH$_c$ to CH$_a$. In addition, while there is little variation in overflow among the different groups for CH$_t$ and CH$_c$, the trends for a vinyl CH bond adjacent to the substituent are just those for the saturated CH. The overflow populations of substituted acetylenes are virtually independent of the substituent.

V. Conclusions

It has been shown in this work that bond moments, bond energies, and certain components of the localized charge distribution energies are indeed transferable from molecule to molecule in a particular way. Specifically, properties of localized charge distributions may be categorized in terms of the types of atoms onto which there is a significant flow of electron density in the bond orbital. These overflow atoms are found to generally occur in pairs which are trans and coplanar to the atoms of the bond. The effect of one pair of overflow atoms is almost independent of the presence of another pair, so that overflow density effects are additive with respect to increasing substitution on the carbon.

The net bond moment is the vector sum of a polarization term (μ_{sp}) and a point charge contribution (μ_{pc}). For CH bonds in hydrocarbons, since there is little charge separation, the polarization term accounts for most of the moment, while the trends in the magnitudes and orientations of the bond moments are strongly dependent on the point charge contribution. In all cases the hydrogen is found to be at the negative end of the dipole.

As expected, the total energies of the localized charge distributions are not very regular; however, the intradistribution part of the energy, R_{ii}, is highly transferable. This is encouraging and one wonders if a similar *ab initio* study would find the total intradistribution energy (not obtainable from INDO) to follow the same behavior. This latter possibility is given added weight by the fact that β_i(CH) are also transferable.

The total energy of a localized charge distribution, e_i, does not correspond to a bond energy in the usual sense (that is, the difference in energy between the molecules and the fragments formed by breaking the bond), but to the total energy of the charge distribution (in this case a CH bond) within the molecular environment. Trends in experimental CH bond energies are, however, well reproduced by that part of the interference energy between the bonded atoms [β_i(CH)], although the magnitudes differ considerably. This supports earlier hypotheses[13,22–26] concerning the importance of the interference energy in chemical binding.

The transferability of β_i(CH) for a given type of overflow atom pairs is also encouraging and, in fact, may indicate why some previous attempts using bond additivity rules for CH bonds have run into trouble. Rules based only on the degree of substitution or type of hybridization on the carbon of the bond[27] are unlikely to be successful since the results of section III indicate that the effect is more subtle.

Finally, it must be noted, in light of the results of paper I[8] of this series, that those relative values of the

---

[27] See, *e.g.*, J. D. Overmars and S. M. Blinder, *J. Phys. Chem.*, **68**, 1801 (1964).

energy quantities quoted in section III which differ only in the second place in electron volts, must be viewed with some degree of caution since the molecular geometries were not optimized for any of the molecules treated here. However, we are very encouraged by the results obtained thus far and are presently analyzing CC bonds in hydrocarbons in the same way. We also are in the process of making models for the LMO's themselves and studying different classes of organic compounds, such as fluorides and carbonyls.

Theoretical Reaction Coordinate for the Methyl Isocyanide Isomerization[1]

Dean H. Liskow, Charles F. Bender, and Henry F. Schaefer III*

Contribution from the Department of Chemistry and Lawrence Berkeley Laboratory, University of California, Berkeley, California 94720.
Received January 14, 1971

Abstract: *Ab initio* self-consistent-field calculations have been carried out to approximately determine the minimum energy path for the $CH_3NC \rightarrow CH_3CN$ reaction. A set of four s and two p functions on C and N and two s functions on H was used. The predicted exothermicity was 17.4 kcal/mol, in reasonable agreement with Benson's empirical estimate of 15 kcal. The calculated barrier height was 58.8 kcal compared to Rabinovitch's experimental value of 38.4 kcal. This difference is ascribed to an expectation that electron correlation will be greater for the transition state than for either CH_3NC or CH_3CN. The calculations differ from the extended Hückel treatment of Van Dine and Hoffmann in that we predict the CH_3 group to remain pyramidal (HCX angle 106°) at the saddle point. The planar CH_3 structure lies 14 kcal higher in energy. The question of changes in "charge" on the methyl carbon is investigated in detail. Mulliken atomic populations suggest that the charge on the methyl carbon at the transition state is intermediate between CH_3NC and CH_3CN. This is completely consistent with the conclusions of Casanova, Werner, and Schuster. However, it is suggested that several other properties (including the potential at each nucleus, the 1s electron binding energies, and the electric field gradients) give a more reliable picture of the changes in electronic structure. These properties suggest that at the transition state there is somewhat more charge on the methyl carbon than in either the product or reactant. The unfavored transition state, in which the CH_3 group is forced to be planar, has a large amount of charge on the methyl carbon, resulting in an electronic structure approaching $[CH_3^+][CN^-]$.

The $CH_3NC \rightarrow CH_3CN$ reaction is one of the simplest examples of a unimolecular isomerization. The kinetics of this reaction have been studied exhaustively by Rabinovitch and coworkers[2,3] over the past decade. Rabinovitch's work has yielded a wealth of information concerning the mechanism of the isomerization, energy transfer, and the suitability of various theoretical models[4] (*e.g.*, RRKM) for describing the kinetics of the reaction. Recently, Harris and Bunker[5] have taken another significant step toward an understanding of the dynamics of the $CH_3NC \rightarrow CH_3CN$ reaction. Using a model potential energy surface, Harris and Bunker[5a] carried out classical trajectory studies[6] of the isocyanide isomerization. Their most important conclusion was that, given an initial internal energy of 150–300 kcal/mol, intramolecular energy transfer into the reaction coordinate probably does not occur for times t less than 10^{-10} sec. In a recent communication,[5b] Harris and Bunker emphasize the non-RRKM behavior of CH_3NC.

It seems clear that an accurate *a priori* potential energy surface for the CH_3CN isomerization would be of great value in providing insight concerning the reaction dynamics. The first step in this direction was taken by Van Dine and Hoffmann,[7] who constructed a CH_3CN potential energy surface from extended Hückel calculations. Van Dine and Hoffmann predicted the saddle point (transition state) to occur for a nearly isosceles CNC triangular arrangement. Their calculated barrier height (activation energy) was 40.8 kcal/mol, in surprisingly good agreement with experiment, 38.4 kcal/mol. Another interesting feature of the Van Dine–Hoffmann calculations is the prediction that the methyl group becomes planar (120° HCH angle) at the saddle point. In the isolated CH_3CN molecule, the HCC angle is 109.5°.

In the present paper, we take a second step toward obtaining a reliable potential surface for $CH_3NC \rightarrow CH_3CN$, a series of nonempirical self-consistent-field calculations. We began this study with the expectation that the Hartree–Fock approximation would be inherently incapable of describing the potential surface in a quantitatively correct manner. In particular, one expects the correlation energy to be significantly greater near the saddle point geometry than for either the reactant CH_3NC or the product CH_3CN.[8] Thus we can

---

[1] Work performed under the auspices of the U. S. Atomic Energy Commission.

[2] (a) F. W. Schneider and B. S. Rabinovitch, *J. Amer. Chem. Soc.*, **84**, 4215 (1962); (b) B. S. Rabinovitch, P. W. Gilderson, and F. W. Schneider, *ibid.*, 87, 158 (1965).

[3] S. C. Chan, B. S. Rabinovitch, J. T. Bryant, L. D. Spicer, T. Fujimoto, Y. N. Lin, and S. P. Pavlou, *J. Phys. Chem.*, **74**, 3160 (1970).

[4] H. S. Johnston, "Gas Phase Reaction Rate Theory," Ronald Press, New York, N. Y., 1966.

[5] (a) H. H. Harris and D. L. Bunker, 161st National Meeting of the American Chemical Society, Los Angeles, Calif., 1971, Physical Chemistry Abstract No. 82; (b) *Chem. Phys. Lett.*, 11, 433 (1971).

[6] M. Karplus in "Molecular Beams and Reaction Kinetics," Ch. Schlier, Ed., Academic Press, New York, N. Y., 1970.

[7] G. W. Van Dine and R. Hoffmann, *J. Amer. Chem. Soc.*, **90**, 3227 (1968).

[8] H. F. Schaefer, "The Electronic Structure of Atoms and Molecules: A Survey of Rigorous Quantum Mechanical Results," Addison-Wesley, Reading, Mass., Feb 1972.